

# Low Power Cylindrical Hall Thruster Performance and Plume Properties

Kevin D. Diamant<sup>1</sup> and James E. Pollard<sup>2</sup>  
*The Aerospace Corporation, P.O. Box 92957, Los Angeles, CA 90009*

Yevgeny Raitses<sup>3</sup> and Nathaniel J. Fisch<sup>4</sup>  
*Princeton University Plasma Physics Laboratory, P.O. Box 451, Princeton, NJ 08543*

**A low power cylindrical Hall thruster (CHT) and fully cylindrical Hall thruster (FCHT) both demonstrated plume divergence reductions of approximately 25% by running a keeper discharge along with the anode discharge. Thruster anode efficiencies varied from approximately 15 to 35% over input powers from 70 to 220 W. A 2 A keeper discharge resulted in an approximately 20% increase in anode specific impulse for both thrusters, and the FCHT specific impulse was, on average, 13% higher than that of the CHT. Both thrusters exhibited mass utilization efficiencies greater than 100% due to generation of multi-charged ions. The quantity of channel erosion products in the plume correlated with that of multi-charged ions.**

## I. Introduction

THE concept of operationally responsive access to space is leading to increased interest in small, low power spacecraft. These severely mass and power limited spacecraft could benefit from the use of low power electric propulsion for orbit maintenance. Hall thrusters may be an attractive option due to their simplicity relative to ion thrusters, and high performance relative to cold gas or electrothermal thrusters.

Annular Hall thrusters have been extensively developed in the power range from approximately 0.5 to 5 kW, with specific impulses from about 1500 to 2000 s, and total efficiencies from 45 to 55%. A number of methodologies are available for scaling Hall thrusters to power levels below a few hundred watts, while attempting to preserve specific impulse and efficiency.<sup>1-6</sup> All face the same challenges, created by the need to reduce channel size to preserve ionization efficiency. Small size leads to difficulty in generation of magnetic fields with appropriate magnitude and topology, and to increased particle losses to chamber walls, with consequent increases in electron transport, heating, erosion, and plume divergence,<sup>7,8</sup> and therefore reduced efficiency, specific impulse, and life. With a few exceptions (BHT-200,<sup>2</sup> KM-37,<sup>7</sup> SPT X-40,<sup>8</sup> SPT-20M6.1<sup>9</sup>), anode efficiencies for annular Hall thrusters operating below 200 W are less than 40%.

Raitses and Fisch developed what they call a cylindrical Hall thruster (CHT), combining the conventional annular design with the simplicity and enhanced volume to surface area ratio of the end-Hall thruster (EHT).<sup>10</sup> The CHT channel features a coaxial region near the anode, followed by a cylindrical region. The coaxial region facilitates ionization, while ion acceleration occurs mainly in the cylindrical region, where there is no inner wall, and consequently reduced particle losses.<sup>11,12</sup> As with the EHT,<sup>13</sup> the magnetic field has substantial axial as well as radial components, with a magnetic mirror in the central portion of the channel. However, in contrast to the EHT, plasma potential measurements in the CHT indicate that the magnetic field lines form equipotential surfaces.<sup>12</sup> Also, the CHT channel is ceramic (boron nitride), while the EHT channel consists largely of the metallic anode.<sup>13</sup> The magnetic mirror in the CHT serves mainly to confine electrons from entering the annular part of the channel.<sup>14</sup> The CHT exhibits quiet operation,<sup>11</sup> and high ionization efficiency.<sup>15</sup> A 3 cm diameter CHT achieved anode efficiencies from 20 to 27% at input powers from 90 to 185 W.<sup>16</sup> More recently, it was found that by "overrunning" the discharge current in 2.6 and 3 cm diameter CHTs, plume divergence was reduced 20-30%, and the ion energy

<sup>1</sup> Senior Member of Technical Staff, Propulsion Science, M2-341, Senior Member AIAA.

<sup>2</sup> Senior Scientist, Propulsion Science, M2-341.

<sup>3</sup> Research Physicist, MS-17, Member AIAA.

<sup>4</sup> Director of Program in Plasma Physics and Professor of Astrophysical Sciences, MS1730, Member AIAA.

distribution was shifted to higher energies.<sup>17</sup> Anode efficiencies of 33-41% (not including power required to overrun the discharge) at 50-175 W were measured with the 2.6 cm thruster.<sup>17</sup>

In this paper we present independent verification of plume narrowing and performance enhancement in the overrun current regime for a 3 cm CHT, and for the same thruster with the annular portion removed (fully cylindrical Hall thruster, or FCHT). The FCHT design was introduced by Raitses and Fisch,<sup>18</sup> and a 5.6 cm diameter version has been developed and studied by Shirasaki and Tahara.<sup>19</sup> We will also present data on ion charge state and erosion species in the plume, and on plasma properties in the near field of the CHT.

## II. Experiment

The 3 cm CHT (Fig. 1) has been described in detail elsewhere.<sup>17,20</sup> The FCHT is the same thruster, modified so that the inner channel wall ends flush with the downstream face of the anode. In all cases the two magnet coils were run in what Smirnov, Raitses, and Fisch refer to as the “direct” configuration, which produces an enhanced axial component of the magnetic field at the outer wall, and a stronger magnetic mirror on the thruster axis.<sup>14</sup> Magnet currents were 2 A except as noted. A commercial hollow cathode (Heatwave Labs model HWPES-250) supplied electrons to the discharge and plume. This cathode consists of a hollow tube with a barium-impregnated porous tungsten emitter, enclosed by a keeper electrode. As in Ref. 17, the overrun current regime was attained by running a keeper discharge in addition to the main discharge to the anode. The cathode keeper exit aperture was located 54 mm radially from thruster centerline, and 20 mm downstream of the thruster exit plane. The angle between the thruster and cathode axes was approximately 40°. Xenon gas was supplied to the anode and cathode by thermal mass flow controllers, calibrated by measuring the pressure rise in a 1-liter volume. The cathode flow rate was 0.2 mg/s in all cases. Testing occurred in a 2.4-m diameter  $\times$  9.8-m long cryopumped vacuum chamber. During thruster operation at a total flow of 0.6 mg/s, chamber pressure (corrected for xenon) was typically  $9 \times 10^{-7}$  Torr.

The thruster was mounted on an inverted pendulum style thrust stand, described in Ref. 21. Ion flux was measured at 2° increments at a radius of 50 cm by a planar probe consisting of a 1.27 cm diameter collector, surrounded by a 2.54 cm outside diameter, 1.32 cm inside diameter guard ring. Collector and guard ring were stainless steel, and both were biased to -20 V with respect to ground. Ion flux was integrated to determine the total beam current and plume divergence. Plume divergence is defined as the half angle containing 90% of the total ion current. The ion energy distribution with respect to ground was measured at 50 cm radius with a retarding potential analyzer, described in Ref. 22. Ion charge state and erosion products were detected with a compact time-of-flight spectrometer, described in Ref. 23. Electron density and temperature, and plasma potential were measured in the plume near field with a single Langmuir probe oriented perpendicular to the ion flow. The probe consisted of a 0.25 mm diameter tungsten wire extending 0.56 mm from the end of a 1.6 mm diameter alumina tube. It was assumed that an ion wake permitted electron collection only on the semicylinder facing the ion flow.<sup>24</sup>

Measurement uncertainties are estimated to be:  $\pm 1^\circ$  for plume divergence,  $\pm 5\%$  for specific impulse,  $\pm 10\%$  for efficiency,  $\pm 20\%$  for electron temperature,  $\pm 1$  V for plasma potential, and  $\pm 50\%$  for electron density.

## III. Results and Discussion

Figure 2 shows ion current density profiles at various keeper currents for the CHT at a main discharge voltage of 250 V and anode flow rate of 0.40 mg/s (discharge currents typically 0.49, 0.51, and 0.53-0.54 A for keeper currents of 0-1, 1.5, and 2-3 A respectively). Figure 3 shows plume divergence for the CHT and FCHT at various operating points. These figures confirm the substantial plume narrowing reported in Ref. 17 for the CHT, and demonstrate that the same effect is present in the FCHT. Plume divergence dropped from an average of 71° with no keeper current, to 55° at 2 A, and 53° at 3 A. Figure 4 shows that a keeper current of 2 A caused CHT primary ion peaks to shift to higher energies, and reduced the number of primary ions at high angles, in agreement with Ref. 17. The ion energy shift was correlated with a shift in the cathode floating potential from about 12-14 V below ground to 1-3 V below ground, equivalent to roughly one half to two thirds of the ion energy shift. Figure 5 shows the CHT running with and without a keeper discharge of 2 A. The keeper discharge affected the appearance of the plume (looks more conical), and caused the cathode to transition from plume mode to spot mode. The plume to spot mode transition is associated primarily with increased plasma density inside the cathode,<sup>25</sup> and reduced voltage between the cathode and the external electron collector,<sup>26</sup> in this case the ion beam. This latter characteristic was evident in the aforementioned shift of cathode floating potential. An explanation for the correlation between cathode plasma density and the full ion energy shift, as well as plume narrowing, is not yet available. Granstedt, Raitses, and Fisch reported CHT plume narrowing resulting from increasing the heating current to a filament cathode beyond that necessary to sustain the discharge,<sup>27</sup> indicating that cathode electron emission capacity is the critical factor, not some other aspect of hollow cathode physics.

The CHT and FCHT have similar anode efficiencies (Fig. 6), and for both thrusters the efficiency improvement created by the narrower, more energetic plume was offset by the power consumed by the keeper discharge (keeper voltage was typically 10 to 12 volts at keeper currents from 1 to 3 A). Presumably, a cathode capable of generating adequate plasma density without a supplemental discharge would achieve the higher efficiencies shown by the open symbols in Fig. 6. Figure 7 shows the benefit of the keeper discharge to CHT and FCHT anode specific impulse, with an average gain of 21% between 0 and 2 A. FCHT specific impulse was, on average, 13% higher than that of the CHT at keeper currents of 0 and 2 A. The possibility of thrust generation by the cathode was investigated by running it alone with a 2 A keeper discharge. Cathode thrust was below the resolution of the stand (0.1 mN). Furthermore, total ion current from the cathode was measured to be approximately 1% of the thruster beam current, and the RPA detected no ions at energies above 20 V, indicating that cathode thrust was probably on the order of 0.01 mN (approximately 0.2% of typical CHT thrust).

Figure 8 shows that mass and current utilization efficiencies for both thrusters were nearly independent of keeper current and discharge voltage, and that mass utilization efficiencies were above 100%. Mass utilization efficiencies were approximately 20% higher for the FCHT, but current utilizations were similar for both thrusters due to the roughly 20% larger discharge current of the FCHT. Ref. 28 reported similar mass utilization efficiencies for a 2.6 cm diameter CHT, and presented evidence indicating that ingestion of cathode flow was not the cause. In this work, a spherical expansion of the cathode flow from the keeper aperture results in an estimated neutral density at the thruster exit plane of about 10 times the vacuum chamber background, leading to a propellant ingestion rate that is approximately 1% of the anode flow rate.

An explanation for high mass utilization in the CHT is provided by the data of Figs. 9 and 10, which show significant populations of multiply charged species at close to the primary ion energy. Ref. 29 suggests that, due to the equipotentiality of magnetic field surfaces, ions born in the near axis region remain at low energy, and are trapped by an ambipolar potential hill that develops in the cylindrical portion due to focusing of fast ions. The increased residence time allows the formation of higher charge states. This mechanism is supported by the data of Fig. 11, which show that the fraction of multiply charged ions increased with decreasing energy-to-charge ratio. Ref. 29 also suggests that the multi-charged ions could erode the central ceramic piece, and indeed Fig. 9 shows that the quantity of  $B^+$  and  $N^+$  (from the BN ceramic) in the plume scaled with that of the multi-charged Xe. Further, the qualitative similarity between the angular distributions of  $B^+$ ,  $N^+$ , and multi-charged Xe (Fig. 10) suggests that they originate from a similar region. The data of Fig. 8 show that the number of multiply charged ions is greater in the FCHT, which could account for its larger specific impulse. Increased generation of multi-charged ions should lead to lower efficiency for the FCHT, but perhaps reduced particle losses due to lack of an inner wall offset the ionization loss.

Langmuir probe data were recorded over a  $15.2 \times 15.2$  cm horizontal grid (2.54 cm step size) in the thruster midplane, centered on the thruster axis, and beginning 1 cm downstream of the exit plane for operation with and without a 2 A keeper discharge. The keeper discharge had a relatively mild effect on electron temperature and plasma potential. Electron temperatures varied from approximately 1 to 2.5 eV (higher temperatures closer to the thruster exit). With the keeper on, temperatures were a few tenths of an eV higher in the region  $\pm 5$  cm radially from the thruster axis, and up to about 5 cm axially downstream of the exit plane. Plasma potentials (referenced to ground) ranged from about 1 to 5 volts, and were 1 to 2 volts higher in most locations with the keeper on. Electron density was much more strongly affected by the keeper discharge, with plume narrowing evident in the data of Fig. 12.

#### IV. Conclusion

With its larger volume to surface area ratio, and simpler magnetic circuit, the cylindrical Hall thruster (CHT) may possess advantages over conventional annular designs when scaling to low power. In this work we have verified that by running a keeper discharge in addition to the anode discharge, the plume divergence of a low power CHT may be decreased by approximately 25%. A similar effect was measured with a fully cylindrical Hall thruster (FCHT), for which the inner wall ends flush with the anode. FCHT efficiency was similar to that of the CHT, but specific impulse was higher, due to increased presence of multi-charged ions. Multi-charged ions caused both thrusters to exhibit mass utilization efficiencies well over 100%, and may be life limiting, since their presence in the plume correlated with that of channel erosion products.

## Acknowledgments

The authors would like to thank Tim Graves for his valuable assistance in the lab, and Artem Smirnov for helpful discussions. This work was supported under The Aerospace Corporation's Independent Research and Development Program.

## References

- <sup>1</sup>Khayms, V. and Martinez-Sanchez, M., "Design of a Miniaturized Hall Thruster for Microsatellites," AIAA 96-3291, 32nd Joint Propulsion Conference, Lake Buena Vista, FL, 1-3 July, 1996.
- <sup>2</sup>Hruby, V., Monheiser, J., Pote, B., Rostler, P., Kolencik, J., and Freeman, C., "Development of Low Power Hall Thrusters," AIAA 99-3534, 30th Plasmadynamics and Lasers Conference, Norfolk, VA, 28 June - 1 July, 1999.
- <sup>3</sup>Warner, N.Z. and Martinez-Sanchez, M., "Design and Preliminary Testing of a Miniaturized TAL Hall Thruster," AIAA 2006-4994, 42nd Joint Propulsion Conference, Sacramento, CA, 9-12 July 2006.
- <sup>4</sup>Battista, F., DeMarco, E., Misuri, T., and Andrenucci, M., "A Review of the Hall Thruster Scaling Methodology," IEPC 2007-313, 30th International Electric Propulsion Conference, Florence, Italy, 17-20 September 2007.
- <sup>5</sup>Belikov, M., Gorshkov, O., Dyshlyuk, E., Lovtsov, A., and Shagayda, A., "Development of Low-Power Hall Thruster with Lifetime up to 3000 Hours," IEPC 2007-129, 30th International Electric Propulsion Conference, Florence, Italy, 17-20 September 2007.
- <sup>6</sup>Ahedo, E. and Gallardo, J., "Scaling Down Hall Thrusters," IEPC 2003-104, 28th International Electric Propulsion Conference, Toulouse, France, 17-21 March 2003.
- <sup>7</sup>Belikov, M., Gorshkov, O., Muravlev, V., Rizakhanov, R., Shagayda, A., and Shnirev, A., "High-Performance Low Power Hall Thruster," AIAA 2001-3780, 37th Joint Propulsion Conference, Salt Lake City, UT, 8-11 July 2001.
- <sup>8</sup>Belikov, M., Gorshkov, O., Rizakhanov, R., Shagayda, A., and Khartov, S., "Hall-Type Low- and Mean-Power Thrusters Output Parameters," AIAA 99-2571, 35<sup>th</sup> Joint Propulsion Conference, Los Angeles, CA, 20-24 June 1999.
- <sup>9</sup>Loyan, A. and Maksymenko, T., "Performance Investigation of SPT-20M Low Power Hall Effect Thruster," IEPC 2007-100, 30th International Electric Propulsion Conference, Florence, Italy, 17-20 September 2007.
- <sup>10</sup>Raitses, Y., Fisch, N.J., Ertmer, K.M., and Burlingame, C.A., "A Study of Cylindrical Hall Thruster for Low Power Space Applications," AIAA 2000-3421, 36<sup>th</sup> Joint Propulsion Conference, Huntsville, AL, July 2000.
- <sup>11</sup>Raitses, Y. and Fisch, N.J., "Parametric Investigations of a Nonconventional Hall Thruster," *Physics of Plasmas*, Vol. 8, No. 5, May 2001, pp. 2579-2586.
- <sup>12</sup>Smirnov, A., Raitses, Y., and Fisch, N.J., "Plasma Measurements in a 100 W Cylindrical Hall Thruster," *Journal of Applied Physics*, Vol. 95, No. 5, March 2004, pp. 2283-2292.
- <sup>13</sup>Kaufman, H.R., Robinson, R.S., and Seddon, R.I., "End-Hall Ion Source," *J. Vac. Sci. Technol. A* 5, July 1987, pp.2081-2084.
- <sup>14</sup>Smirnov, A., Raitses, Y., and Fisch, N.J., "The Effect of Magnetic Field on the Performance of Low-Power Cylindrical Hall Thrusters," IEPC-2005-099, 29<sup>th</sup> International Electric Propulsion Conference, Princeton, NJ, 2005.
- <sup>15</sup>Smirnov, A., Raitses, Y., and Fisch, N., "Enhanced Ionization in the Cylindrical Hall Thruster," *Journal of Applied Physics*, Vol. 94, No. 2, July 2003, pp. 852-857.
- <sup>16</sup>Polzin, K.A., Markusic, T.E., Stanojev, B.J., Dehoyos, A., Raitses, Y., Smirnov, A., and Fisch, N.J., "Performance of a Low-Power Cylindrical Hall Thruster," *Journal of Propulsion and Power*, Vol. 23, No. 4, July-August 2007, pp. 886-888.
- <sup>17</sup>Raitses, Y., Smirnov, A., and Fisch, N., "Enhanced Performance of Cylindrical Hall Thrusters," *Applied Physics Letters*, 90, 221502, 2007.
- <sup>18</sup>Raitses, Y. and Fisch, N.J., "Cylindrical Geometry Hall Thruster," US Patent No.: 6,448,721 B2, September 2002.
- <sup>19</sup>Shirasaki, A. and Tahara, H., "Operational Characteristics and Plasma Measurements in Cylindrical Hall Thrusters," *Journal of Applied Physics* 101, 073307 (2007).
- <sup>20</sup>Smirnov, A., Raitses, Y., and Fisch, N., "Parametric Investigation of Miniaturized Cylindrical and Annular Hall Thrusters," *Journal of Applied Physics*, Vol. 92, No. 10, November 2002, pp. 5673-5679.
- <sup>21</sup>Diamant, K.D., Brandenburg, J.E., Cohen, R.B., and Kline, J.F., "Performance Measurements of a Water Fed Microwave Electrothermal Thruster," AIAA 2001-3900, 37th Joint Propulsion Conference, Salt Lake City, UT, 8-11 July 2001.
- <sup>22</sup>Pollard, J.E. and Diamant, K.D., "Hall Thruster Plume Shield Wake Structure," AIAA 2003-5018, 39<sup>th</sup> Joint Propulsion Conference, Huntsville, AL, 20-23 July 2003.
- <sup>23</sup>Pollard, J.E., Diamant, K.D., Khayms, V., Werthman, L., King, D.Q., and de Grys, K.H., "Ion Flux, Energy, and Charge-State Measurements for the BPT-4000 Hall Thruster," AIAA 2001-3351, 37th Joint Propulsion Conference, Salt Lake City, UT, 8-11 July 2001.
- <sup>24</sup>de Boer, P.C.T., "Electric Probe Measurements in the Plume of an Ion Thruster," *Journal of Propulsion and Power*, Vol. 12, No. 1, January-February 1996, pp. 95-104.
- <sup>25</sup>Mandell, M. and Katz, I., "Theory of Hollow Cathode Operation in Spot and Plume Modes," AIAA 94-3134, 30<sup>th</sup> Joint Propulsion Conference, Indianapolis, IN, 27-29 June 1994.
- <sup>26</sup>Domonkos, M., Patterson, M., and Gallimore, A., "Low-Current, Xenon Orificed Hollow Cathode Performance for In-Space Applications," *Journal of Propulsion and Power*, Vol. 19, No. 3, May-June 2003.
- <sup>27</sup>Granstedt, E., Raitses, Y., and Fisch, N.J., "Cathode Effects in Cylindrical Hall Thrusters," *Journal of Applied Physics* (to be published).

<sup>28</sup>Raitses, Y., Smirnov, A., Granstedt, E., and Fisch, N.J., "Optimization of Cylindrical Hall Thrusters," AIAA 2007-5204, 43<sup>rd</sup> Joint Propulsion Conference, Cincinnati, OH, 8-11 July 2007.  
<sup>29</sup>Smirnov, A., Raitses, Y., and Fisch, N.J., "Electron Transport and Ion Acceleration in a Low-Power Cylindrical Hall Thruster," AIAA 2004-4103, 40<sup>th</sup> Joint Propulsion Conference, Fort Lauderdale, FL, 11-14 July 2004.

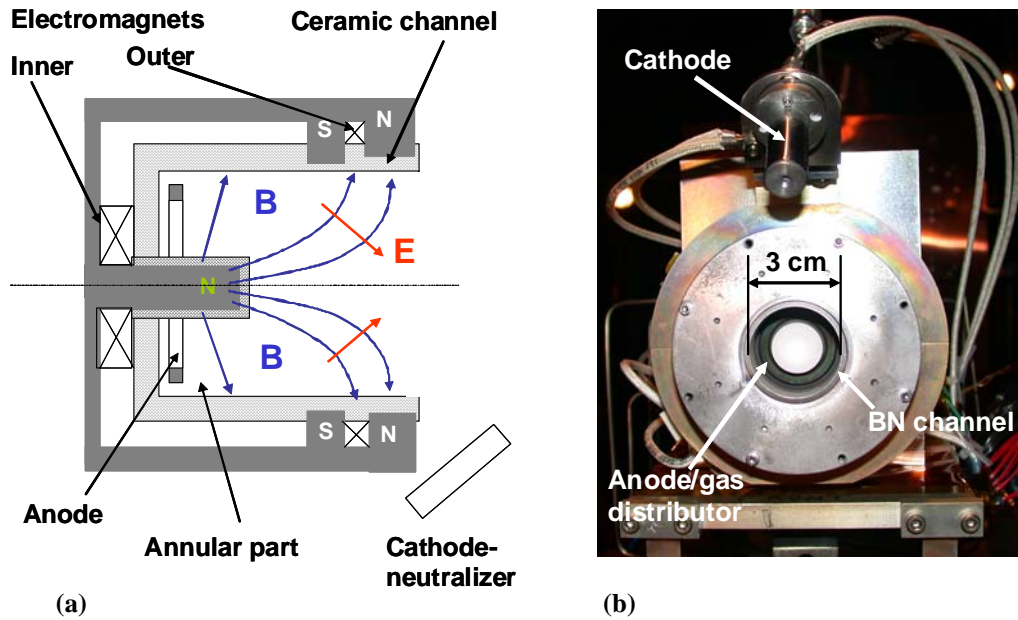


Figure 1. (a) CHT schematic (from Raitses, Smirnov, Granstedt, and Fisch, presentation at 43<sup>rd</sup> Joint Propulsion Conference, Cincinnati, OH, 2007). (b) 3 cm CHT.

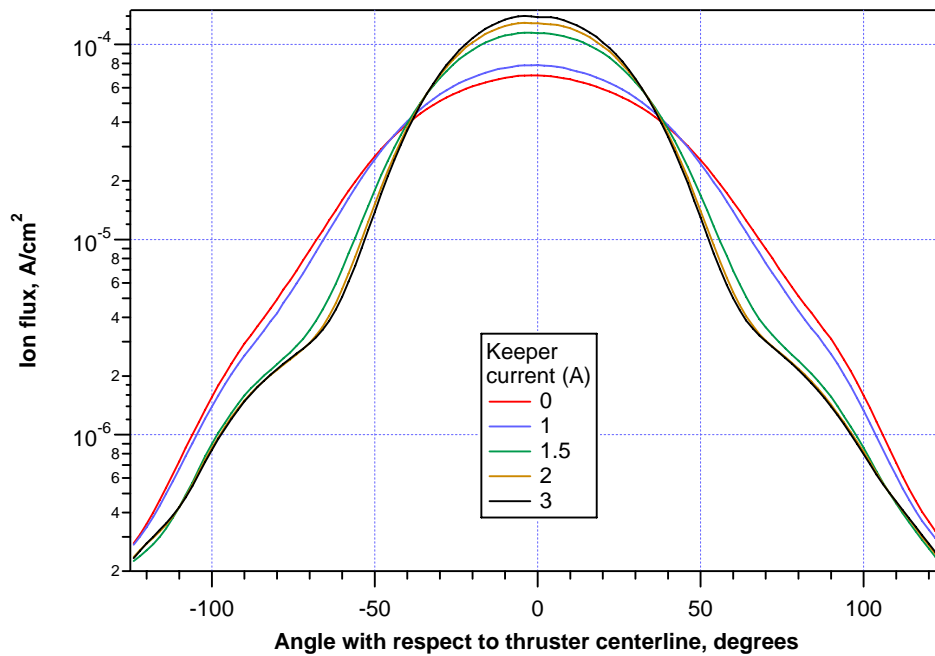


Figure 2. CHT ion flux at 50 cm radius for various keeper currents. Main discharge 250 V, 0.40 mg/s.

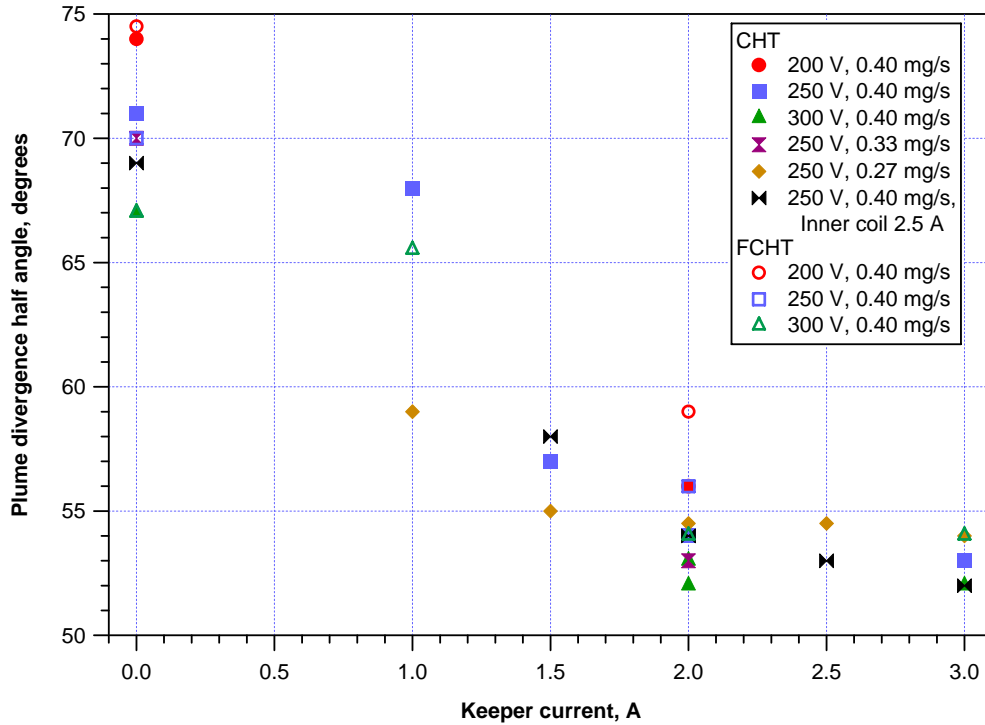


Figure 3. Plume divergence.

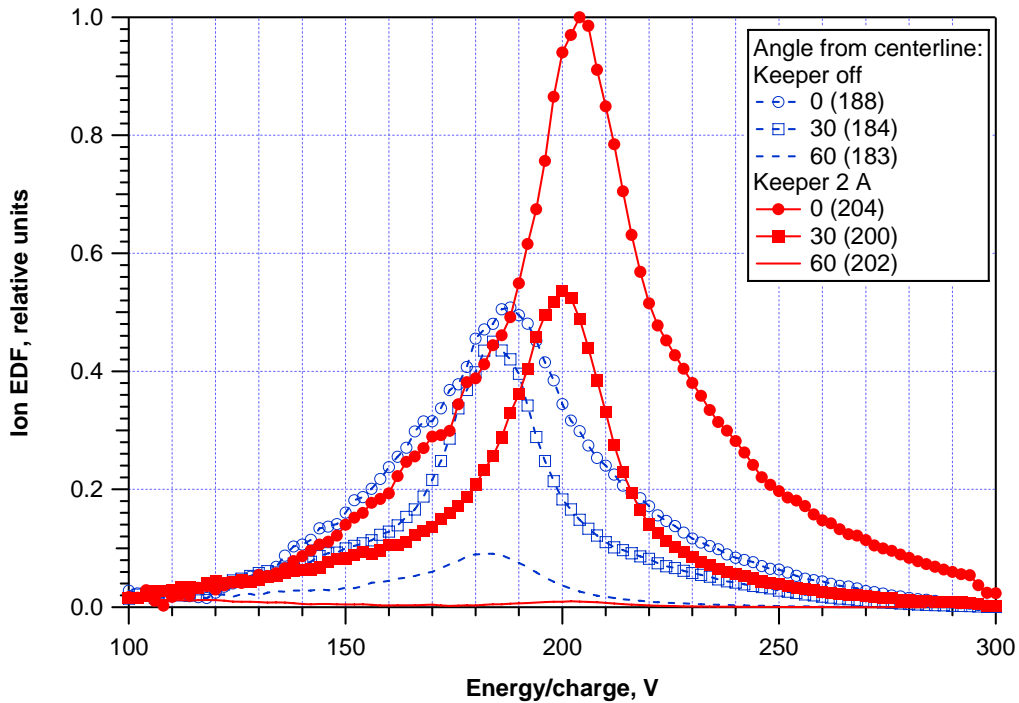


Figure 4. CHT ion energy distribution, 250 V, 0.40 mg/s. Peak center voltages are listed in parentheses in the legend.

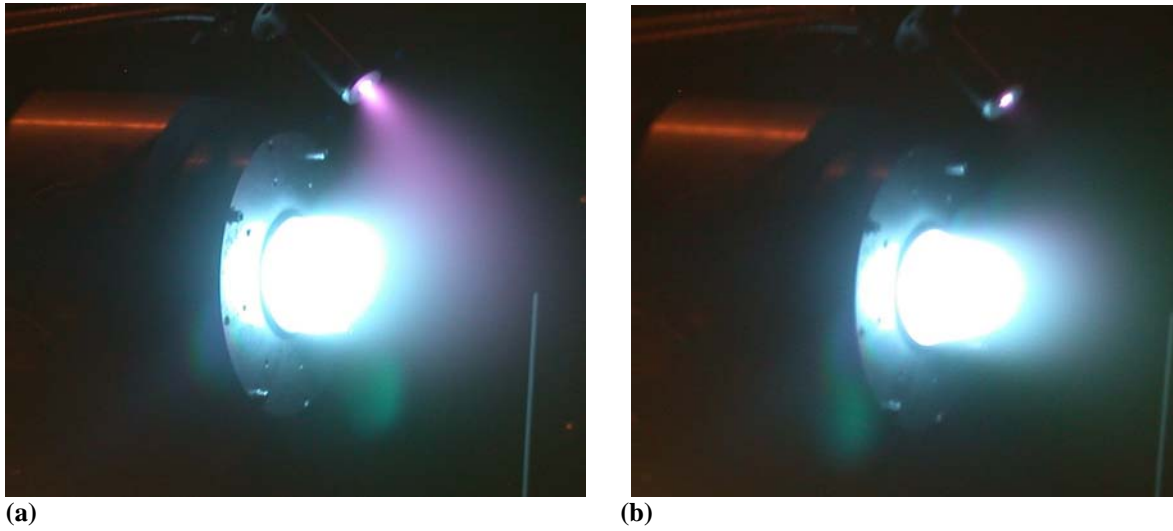


Figure 5. CHT firing, 250 V, 0.40 mg/s (a) keeper off, (b) keeper 2 A.

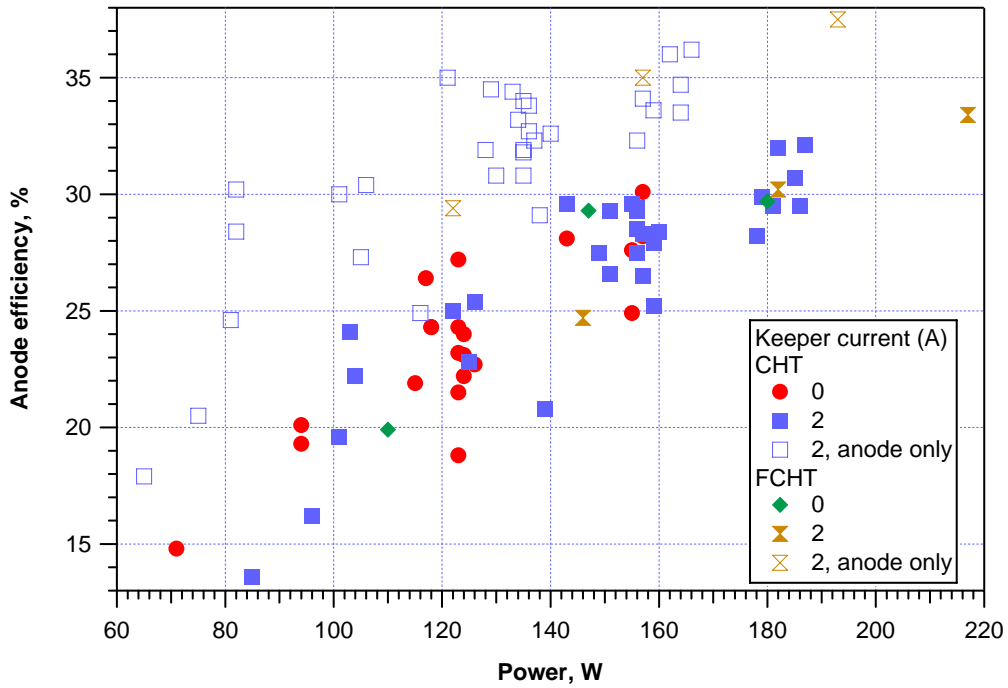


Figure 6. Anode efficiency, magnet power not included. CHT was operated at discharge voltages from 150 to 300 V, and anode mass flow rates from 0.28 to 0.40 mg/s. FCHT was operated at 200 to 300 V, and 0.40 mg/s. Open symbols marked “anode only” represent the same operating conditions as the closed symbols of the same shape and color, except that the keeper power is not included in the calculation of efficiency.

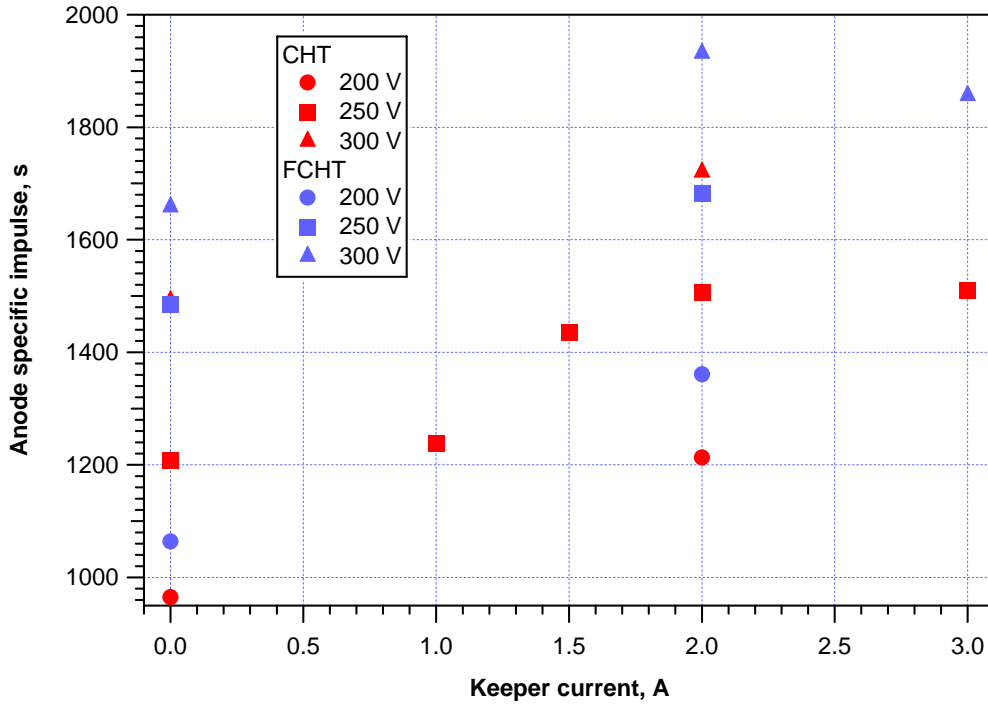


Figure 7. Anode specific impulse, 0.40 mg/s.

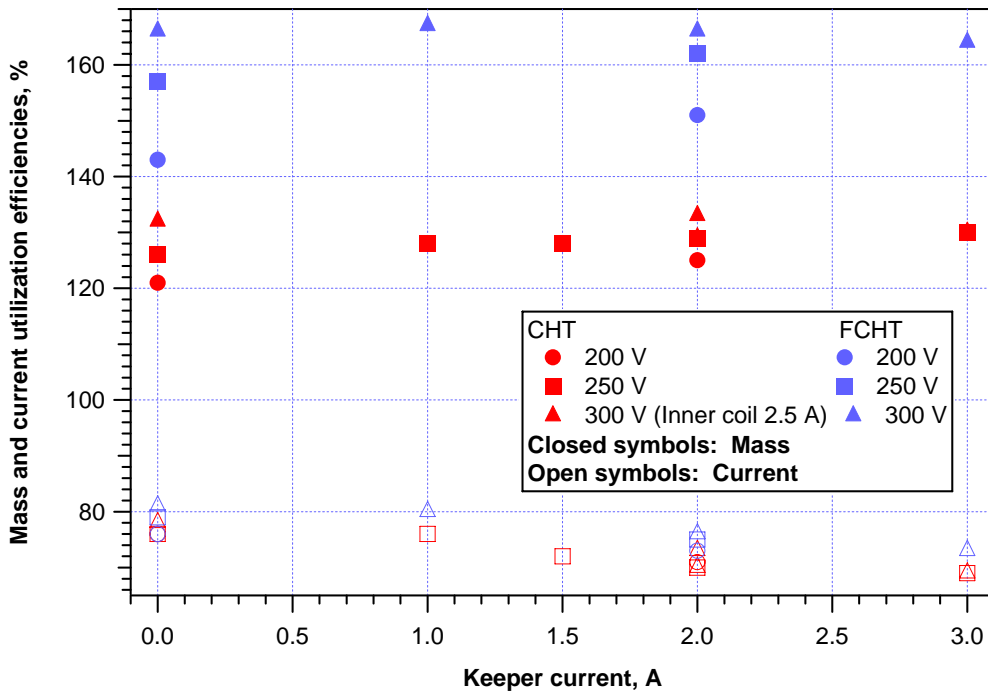


Figure 8. Mass and current utilization efficiencies, 0.40 mg/s.

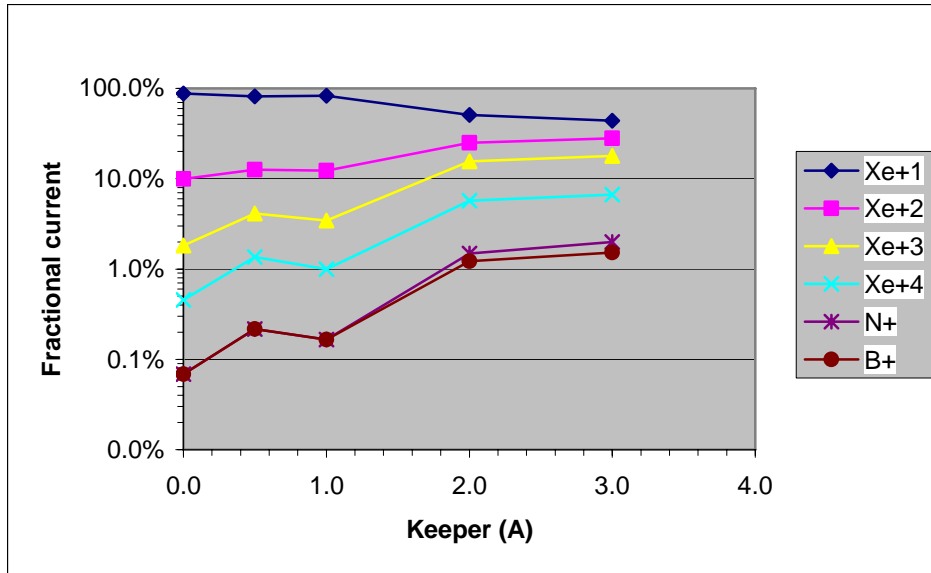


Figure 9. Effect of keeper current on CHT xenon charge state and erosion products. 250 V, 0.40 mg/s, 40° from thruster centerline, energy-to-charge ratio = 223 V.

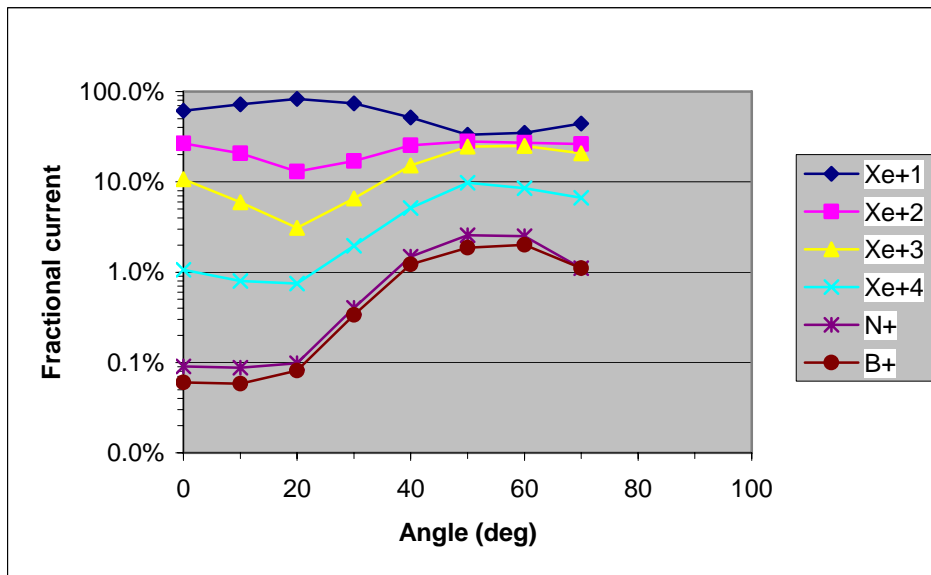


Figure 10. CHT xenon charge state and erosion products vs angle at 2 A keeper current. 250 V, 0.40 mg/s, energy-to-charge ratio = 223 V.

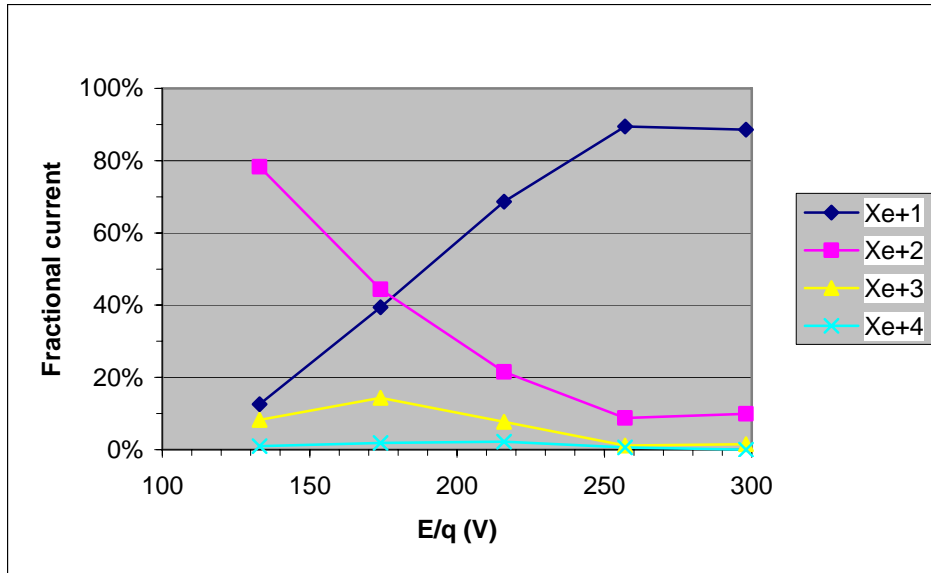
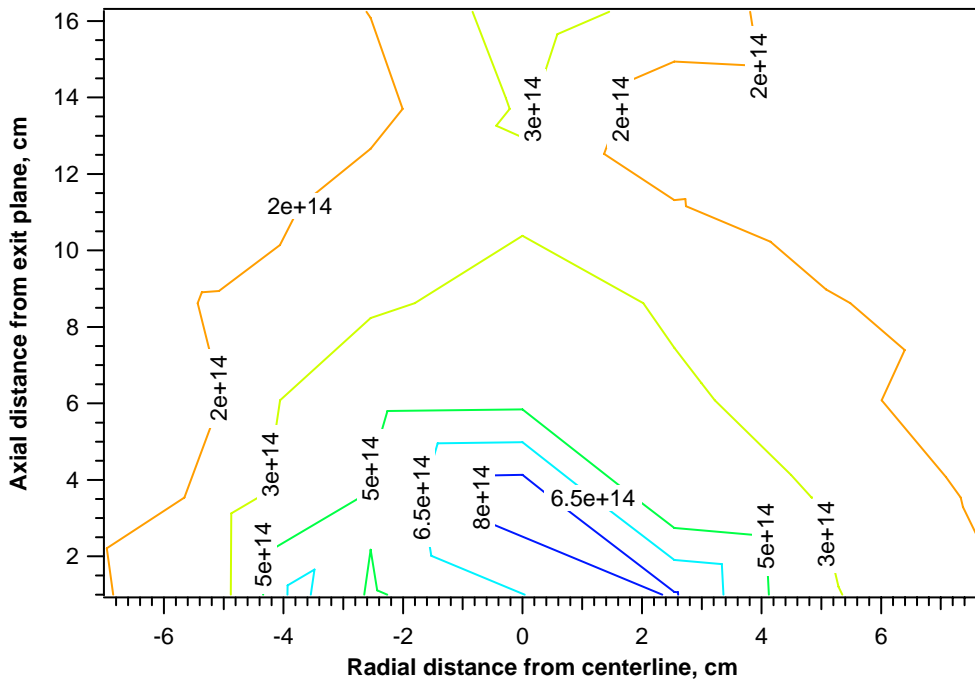
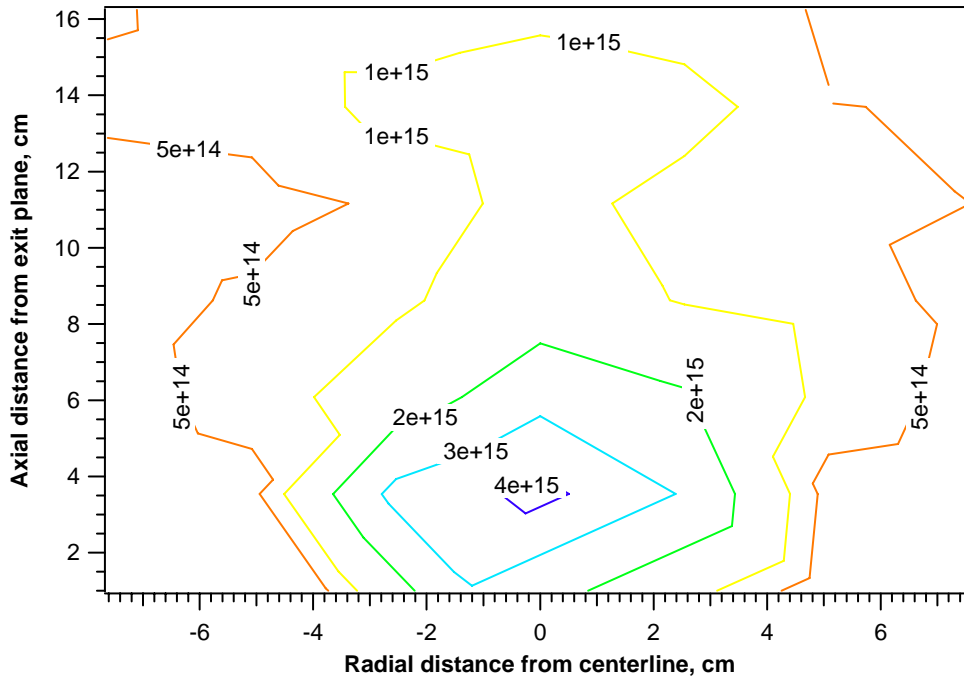


Figure 11. CHT ion charge state vs energy-to-charge ratio for 2 A keeper current. 250 V, 0.40 mg/s, 30° from thruster centerline.



(a)



(b)

Figure 12. Electron density,  $\text{m}^{-3}$  for CHT operation at 250 V, 0.40 mg/s (a) no keeper discharge, (b) 2 A keeper discharge.